



Testing resonant scalar top quark pair production at next-to-leading order in QCD

written by: Felix Hagemann, Technische Universität Berlin

supervised by: Alexander Grohsjean, CMS, DESY

September 7, 2017

Abstract

Many scenarios beyond the standard model predict scalar and pseudoscalar production and decay into a top-antitop-pair. In order to find evidence for the existence of additional scalars in experimental data it is essential to understand the interference between scalar and standard model top pair production and its characteristic peak-dip structures in particular. Interference effects between scalar top pair production and standard model are known at leading order. However, QCD corrections at next-to-leading order are known to have a large impact on both signal and background. In this report an effective field theory approach considering a point-like interaction between gluons and scalar particles presented by *Franzosi et al.* [1] is used to study interference effects between resonant scalar top pair production and standard model background. The characteristic peak-dip structure of the computed interference lineshape is presented and in good agreement with theoretical predictions. Moreover, the influence of an additional phase to describe the absorptive part of the top loop in the resolved case is discussed.

Contents

1	Introduction	1
2	Theoretical setup	2
2.1	Two-Higgs-Doublet Model	2
2.2	Interference effects between signal and SM background	2
2.3	Effective field theory	3
2.4	Next-to-leading order corrections	4
3	Technical setup	5
3.1	MADGRAPH5_AMC@NLO	5
3.2	Phase calculation	6
4	Lineshape computation	7
4.1	Benchmark	7
4.2	Analysis	7
4.3	Results	8
5	Conclusion	10
6	Acknowledgements	10

1 Introduction

The discovery of the Higgs boson at the LHC in 2012 [2, 3] expanded the standard model (SM) by a scalar particle, providing a possible explanation for particle mass acquisition due to electroweak symmetry breaking. Although there are no hints about the presence of additional Higgs bosons so far, many physicists believe in the existence of more heavy scalar particles that may extend the standard model at some point.

For instance, the two-Higgs-doublet model predicts four additional Higgs bosons. For Higgs bosons heavier than twice the top rest mass, one possible way to find proof for an extended scalar sector would be resonant scalar top pair production. Being the heaviest fermion of the standard model and strongly coupling to the Higgs boson, the top quark may play an important role in finding evidence for physics beyond the standard model (BSM).

The challenge is that top pair production can be initiated by gluons also, which will lead to large background that needs to be considered when making predictions about signal lineshapes. Understanding the influence of interference effects on the signal lineshapes is crucial. In order to be making precise predictions high accuracy is needed. Thus, it is necessary to do complete and precise calculation, avoiding numerous approximations and including higher orders of perturbation.

Scalar production processes at leading order (LO) involve heavy quark loops to induce the vertex between gluon and scalar particles. In this report, a full calculation of resonant scalar top pair production will be tested at next-to-leading order (NLO) accuracy in QCD using an effective field theory (EFT) approach, supposing a point-like gluon to Higgs coupling described by a heavy vector-like fermion [1].

This approach is only valid when the mediation particle is heavier than half the Higgs mass. Studying the case in which the top loop is resolved, the EFT approach can be expanded, by adding an additional phase representing the absorptive part of the ggH -vertex that is not captured in the calculation, to obtain Born-improved predictions. The resulting interference and signal lineshapes will be discussed qualitatively and quantitatively in this report.

The report is organized as follows: a general overview about the perturbative calculation at NLO and the EFT is given in Section 2. A description of the technical setup is given in Section 3. In Section 4 the benchmark, analysis and results to compute interference and signal lineshapes are shown and discussed. Finally, the conclusion is presented in Section 5.

2 Theoretical setup

2.1 Two-Higgs-Doublet Model

Discovering the Higgs boson at the LHC was the first step to combining the scalar sector with the standard model. However, some scenarios beyond the standard model predict extended scalar sectors, allowing the existence of multiple heavier scalar particles.

One possible scenario is based on the two-Higgs-doublet model (2HDM) [4]. Introducing a second $SU(2)_L$ doublet Φ_2 gives rise to five physical Higgs bosons: one light (heavy) neutral, CP-even state h (H); one neutral, CP-odd state A ; and two charged Higgs bosons H^\pm . The properties of this model are given by the vacuum expectation value $\tan\beta$, the mixing angle α and the Higgs masses $m_h, m_H, m_A, m_{H^\pm}, m_{12}^2$ with the convention $0 \leq \beta - \alpha \leq \pi$ and $0 \leq \beta \leq \pi/2$.

The decay of the standard model 125 GeV Higgs boson to top quarks is very unlikely due to the small mass of the Higgs boson compared to the mass of a top quark pair of around 345 GeV. Therefore, studying possible scenarios of resonant scalar top pair production could play a key role in finding additional heavier scalar particles.

2.2 Interference effects between signal and SM background

Expanding the standard model by scenarios beyond the standard model, the overall amplitude can be obtained by adding the standard model amplitude \mathcal{M}_{SM} to the one of the new model \mathcal{M}_{BSM} . Squaring the amplitudes as shown in Eq. (2.1), one gets three contributions to the total cross section: background, signal and interference.

$$\underbrace{|\mathcal{M}_{\text{SM}} + \mathcal{M}_{\text{BSM}}|^2}_{\text{background \& signal}} = \underbrace{|\mathcal{M}_{\text{SM}}|^2}_{\text{background}} + \underbrace{|\mathcal{M}_{\text{BSM}}|^2}_{\text{signal}} + \underbrace{2 \text{Re}(\mathcal{M}_{\text{SM}} \mathcal{M}_{\text{BSM}}^*)}_{\text{interference}} \quad (2.1)$$

In this framework the signal refers to the resonant scalar top pair production while the background refers to pure SM top pair production. Fig. 1 shows LO Feynman diagrams of both signal and background top pair production.

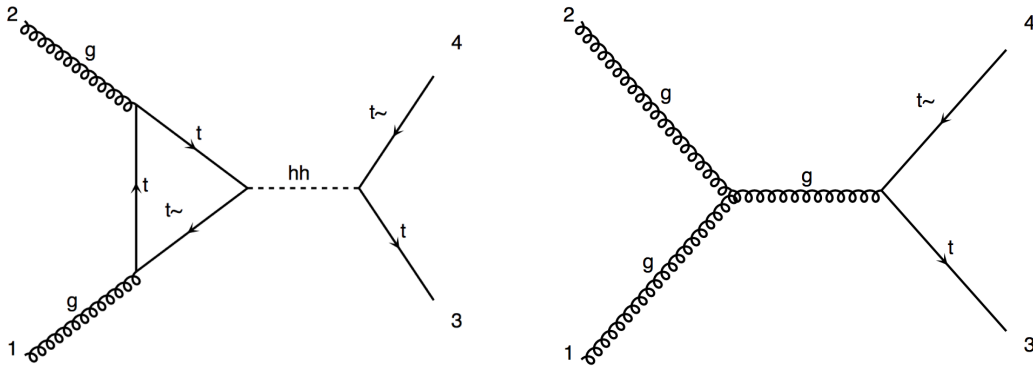


Figure 1: LO Feynman diagrams of scalar top pair production (left) and one of the possible SM background diagram (right).

2.3 Effective field theory

Including NLO corrections to the event generation and performing complete calculations will lead to two-loop virtual diagrams. The computation of these processes can be challenging due to many different scales involved. One possible way to perform the exact computation at NLO is to embed the calculations into EFT introducing a vector-like fermion as detailed in Ref. [1].

Describing the loop-induced ggH -vertices by the new introduced mediation particle does not change the lineshape of the signal at leading order, as can be seen in Fig. 2 assuming a mass of the mediation particle of $m_F = 500$ GeV. The corresponding Feynman diagrams are shown in Fig. 3. The EFT is in good agreement with the exact one-loop calculation and offers the possibility to compute exact NLO corrections in the unresolved case, where the ggH -vertex is induced by particles with masses higher than $m_H/2$.

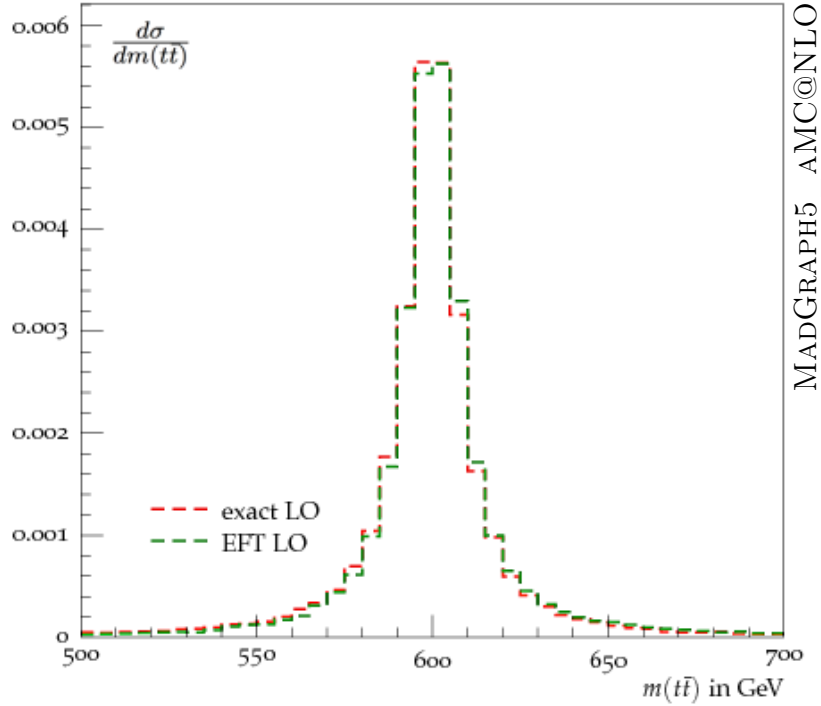


Figure 2: Comparison between the signal obtained by the exact calculation and the calculation in EFT with for a scalar particle with mass $m_H = 600$ GeV and width $\Gamma_H = 15$ GeV, assuming a mediation particle mass of $m_F = 500$ GeV.

Only looking at the resolved case where the ggH -vertex is induced by top quarks with masses $m_F = 172.5$ GeV smaller than $m_H/2$, the EFT is not valid anymore. For instance, it does not capture the absorptive part of the top quark loop which needs to be taken into account when computing the lineshape. That leads to the fact that the amplitudes generated from the EFT and the resolved top-loop become zero at different phase-space points.

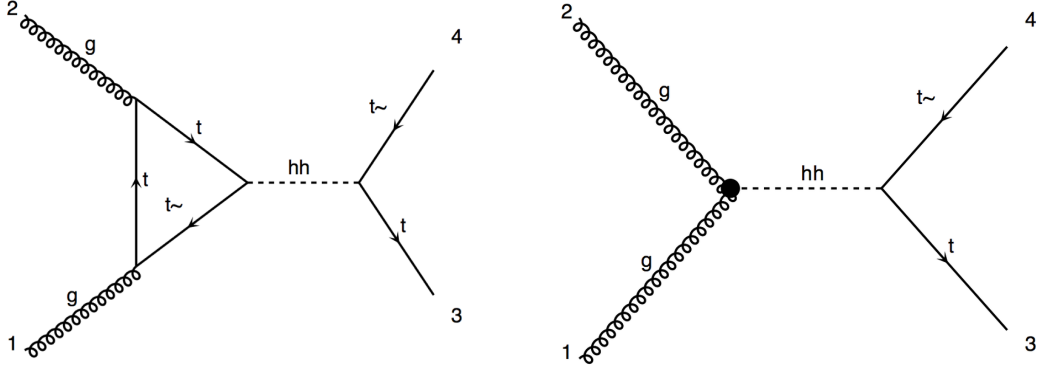


Figure 3: Feynman diagrams for the leading order scalar production and decay to top quarks with resolved top loop (left) and described by an effective field (right).

This can be prevented by introducing a phase in the EFT amplitude resembling the absorptive behaviour of the top loop, as suggested in [1]. Ensuring the amplitude ratio to be finite at all phase space points and performing an event-by-event reweighting at Born level [5] will lead to exact results at LO and Born-improved results at NLO.

2.4 Next-to-leading order corrections

The interference between scalar production and SM background and its effect on the signal lineshape is known at LO. However, NLO corrections in QCD (as shown in Fig. 4) play an important role in making accurate predictions about the interference contribution to the signal lineshape. Fig. 5 shows the pure signal of scalar production computed using the previously discussed EFT approach at LO and NLO normalized to their cross section. It can easily be seen that NLO corrections increase the cross section drastically for the signal, but do not significantly change the lineshape.

Regarding the interference, NLO corrections might change not only the cross section value, but also the lineshape in respect to the exact LO calculations. These effects are about to be tested with the following setup.

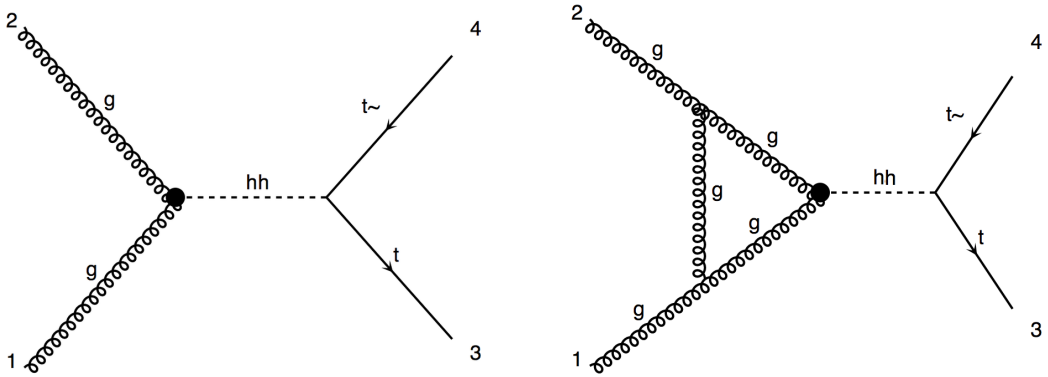


Figure 4: Feynman diagrams for the LO scalar production and decay to top quarks (left) and possible NLO corrections (right).

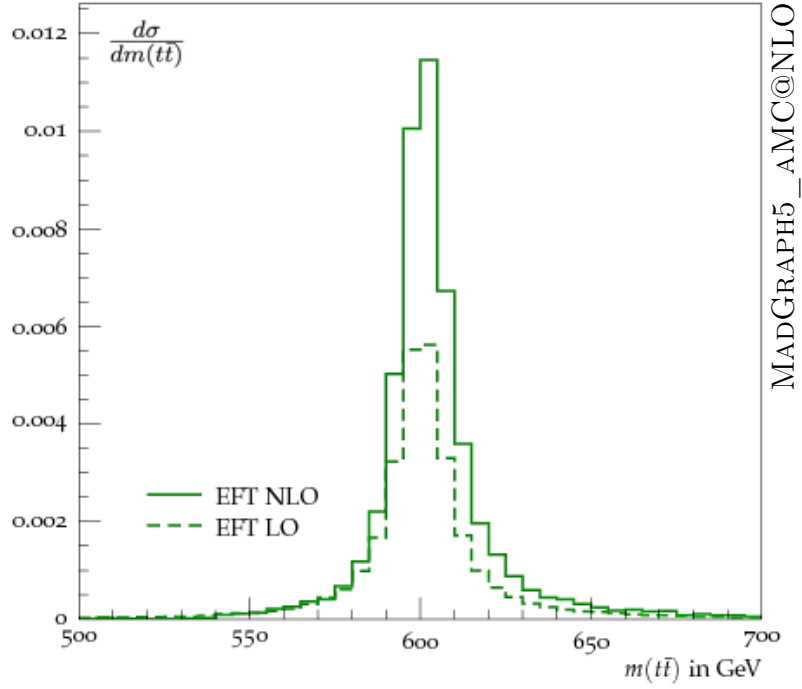


Figure 5: Scalar production signal lineshape calculated by using the EFT approach for a scalar particle with mass $m_H = 600$ GeV and width $\Gamma_H = 15$ GeV normalized to the cross section.

3 Technical setup

3.1 MadGraph5_aMC@NLO

To generate the events and calculate the cross sections MADGRAPH5_AMC@NLO version 2.4.2 [6] was used. The UFO model file this report is based on is **AHttbar** [1]. This file contains the heavy scalar and pseudoscalar particle postulated by the 2HDM and embeds the calculation in the EFT as explained earlier.

In order to perform the calculations, several input parameters need to be given. Besides the parameters describing the 2HDM explained in Section 2.1, additional parameters describing the EFT are needed. These include the Higgs-top Yukawa couplings of both scalar and pseudoscalar particle y_t and \tilde{y}_t , as well as the Higgs loop-inducing fermion Yukawa couplings y_F and \tilde{y}_F respectively, as rescalings of the SM Higgs top Yukawa coupling. In addition, the EFT operator coefficients describing the interactions in gluon-scalar vertices C_{HG} , gluon-pseudoscalar vertices C_{AG} and gluon-top vertices C_{tG} .

In the top-loop resolved case, the Higgs-fermion Yukawa coupling constant is set to $y_F = y_t/\sqrt{2}$ and $\tilde{y}_F = \tilde{y}_t/\sqrt{2}$ respectively and the additional phase $(a + bi)$ describing the absorptive part of the top loop can be handed over.

Two files in the MADGRAPH5_AMC@NLO source code were modified for the event generation: the line `self['loop_diagrams'] = newloopselection` was removed from `madgraph/loop/loop_diagram_generation.py` in order to obtain all the virtual loop corrections and the `Error #4` in `set_matrices` as well as the `Error #6` in `check_mc_matrices` were removed from `Template/NLO/Subprocesses/montecarlocounter.f`.

In the process of producing the gridpack, the helicity amplitude routines were written by ALOHA [7], the width and branching fractions of the top quark and heavy Higgs bosons were computed with FEYNRULES [8] and the decay was simulated using MADSPIN [9].

3.2 Phase calculation

The phase added to the operator coefficients $C_{AG} \rightarrow (a + bi) \times C_{AG}$ to capture the absorptive part of the resolved top loop can be obtained at Born level by plotting analytical expressions for the signal over background ratio [10]. The parameters a and b are chosen in the way that the corresponding interference line from exact and top-loop calculation cross zero at the same point and have the same slope accordingly. Fig. 6 shows the impact of the additional phase to the lineshape obtained by the EFT approach. It can clearly be seen that the interference lineshape obtained by phase improved EFT and exact calculation are almost identical and can be used to predict the interference lineshape at NLO. Small differences between these two lines can be compensated by implementing an event-by-event Born-reweighting.

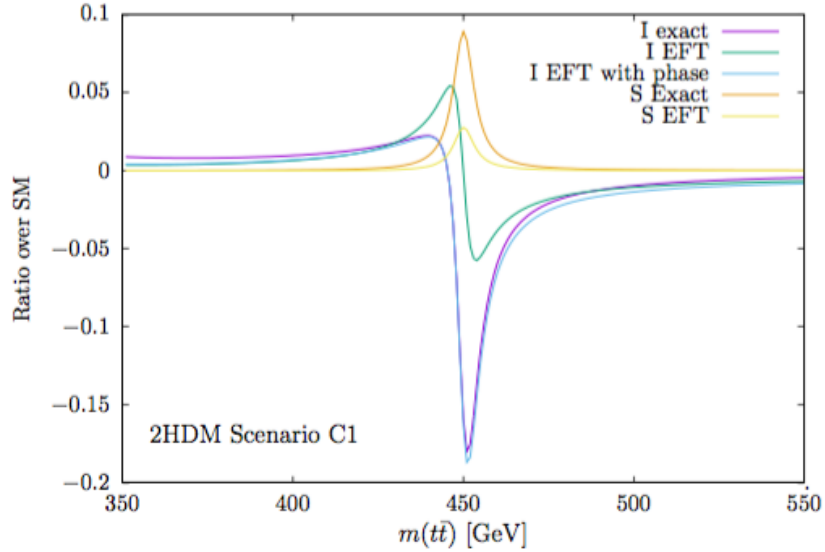


Figure 6: Signal and interference ratio over background at Born level doing exact computation and using EFT with and without an additional phase [1].

4 Lineshape computation

4.1 Benchmark

The benchmark used in this report to test pseudoscalar production and decay to top quarks is similar to the benchmark C1 shown in [1]. The input parameters to define the properties of the 2HDM, Yukawa couplings and the EFT are the following:

$$\begin{array}{lll}
 \tan \beta = 2.0 & y_t = -0.5 & \frac{C_{HG}}{\Lambda} = 4.73 \times 10^{-6} \text{ GeV}^{-1} \\
 \sin(\beta - \alpha) = 1.0 & \tilde{y}_t = 0.5 & \frac{C_{AG}}{\Lambda} = -6.49 \times 10^{-6} \text{ GeV}^{-1} \\
 m_H = 300 \text{ GeV} & y_F = -0.354 & \frac{C_{tG}}{\Lambda} = 9.56 \times 10^{-9} \text{ GeV}^{-1} \\
 m_A = 450 \text{ GeV} & \tilde{y}_F = 0.354 & a + bi = 1.06614 + 1.17661i
 \end{array}$$

To generate the events the NLO NNPDF3.0 parton distribution functions [11] are chosen. Furthermore, the complex mass scheme [12] is used to include the width of the heavy scalar and pseudoscalar particle in the calculations. The additional phase describing the absorptive part of the top loop is set to the default value of the model file.

As the mass of the scalar does not lie above the rest mass of the top pair $2m_t = 345.0 \text{ GeV}$, only pseudoscalar resonances decaying into top-antitop pairs are expected.

4.2 Analysis

MADGRAPH5_AMC@NLO is only able to compute square amplitudes so far. As shown in Eq. (2.1), the square amplitude of a sample combining both signal and background events consists of background, signal and interference terms.

In order to obtain the interference term it would be possible to generate a sample combining the model and background and subtracting background and signal from this sample. However, this involves the generation of three samples, each underlying statistical fluctuations.

Another possible approach to compute the interference lineshape is to generate two samples: one adding and one subtracting the new model from the SM background. This can be achieved by setting the parameter `cc` to `+1` or `-1` respectively. By subtracting these two samples from one another the pure background and signal terms cancel and only the interference term remains.

$$|\mathcal{M}_{\text{SM}} + \mathcal{M}_{\text{BSM}}|^2 - |\mathcal{M}_{\text{SM}} - \mathcal{M}_{\text{BSM}}|^2 = 4 \text{Re}(\mathcal{M}_{\text{SM}} \mathcal{M}_{\text{BSM}}^*) \quad (4.1)$$

This will be the method used in this framework to generate the interference lineshape.

4.3 Results

Generating two samples, one adding the scalar production contribution to the SM background and one subtracting it, one can obtain the invariant mass distribution shown in Fig. 7 using the Rivet analyzer tool [13]. For the LO sample one million events were generated whilst for the NLO sample three million events were produced to minimize fluctuations due to low statistics.

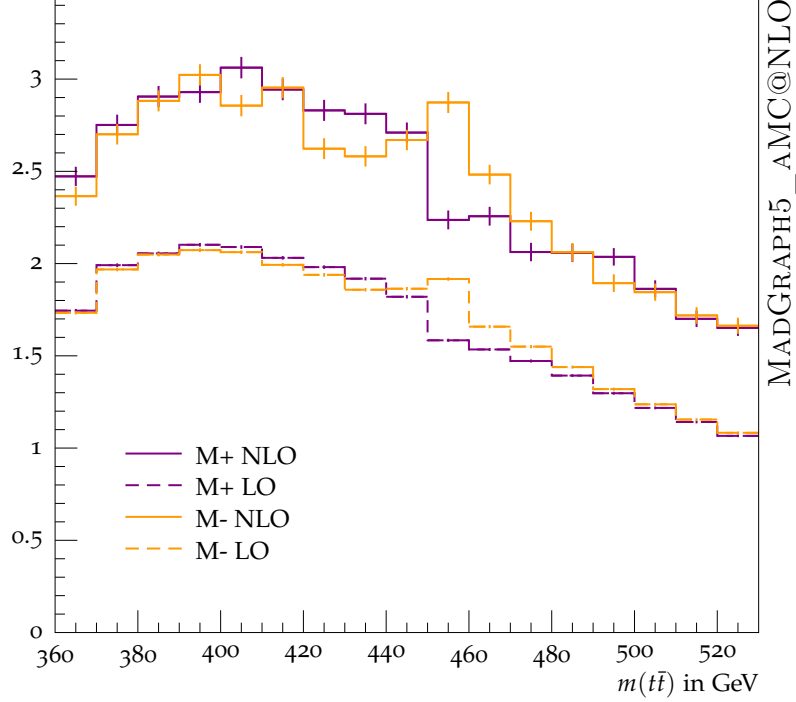


Figure 7: Invariant mass distribution of scalar top pair production samples containing both signal and background by using positive couplings and negative couplings at both LO and NLO and their statistical uncertainties.

First of all, one can clearly see that the interference cannot be neglected in resonant scalar top pair production. Otherwise, both samples would show the same behaviour.

The distribution can be divided in two regions: one around the resonant mass of 450 GeV and one further away from the resonance. In the resonant region, both samples differ significantly from each other, implying strong interference effects at both LO and NLO. Further away from the resonant region, the shape of the distribution for both samples approach each other, indicating smaller interference effects. At LO both samples approach the same shape for small and large top pair invariant masses whilst the NLO samples underlie statistical fluctuations which causes both shapes to vary from one another.

The fact that the difference between both samples at 400 GeV exceeds the statistical uncertainties implies that more samples are needed to obtain a proper lineshape prediction, as seen at LO.

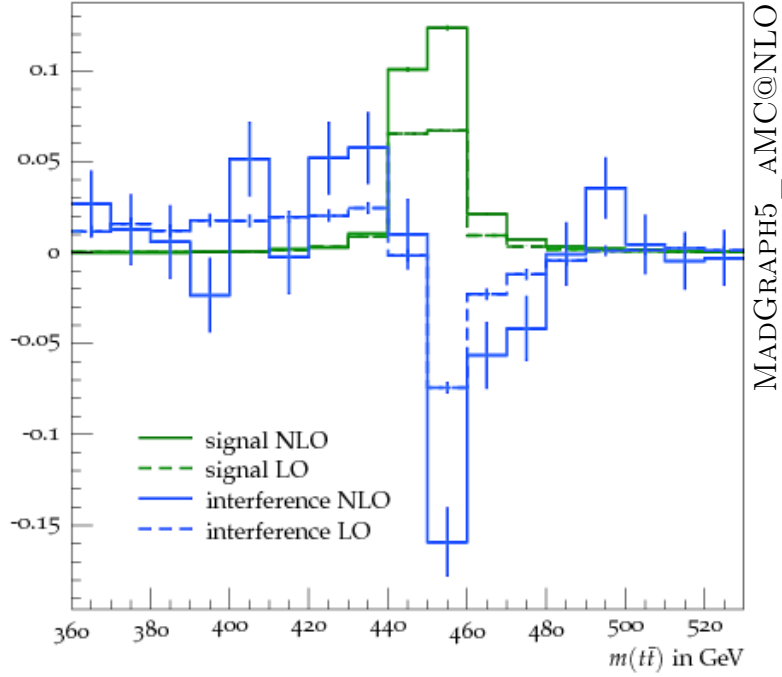


Figure 8: Signal and interference computed at LO and NLO, normalized to the fixed order NLO lineshape and their statistical uncertainties.

Subtracting both samples from one another and dividing by a factor of 2, the interference lineshape shown in Fig. 8 is obtained. As discussed before, at low and high $m(t\bar{t})$ the interference lineshape underlies large statistical fluctuations that impedes making accurate prediction further away from the resonant region. In the region around the resonant mass the peak-dip structure of the interference line can be observed, the obtained lineshape is in good agreement with Ref. [1].

However, there are some differences regarding the cross section values computed at fixed order. Tab. 1 shows the cross sections for background, interference and signal obtained in this framework comparing them to the cross section calculated by *Franzosi et al.* [1].

It can be seen that the values for the different cross section contributions computed in this framework differ from the comparative values. This is due to the fact that for the sample generation the default phase for simulating the top loop absorption was used.

	σ_{LO}	$\tilde{\sigma}_{\text{LO}}$	σ_{NLO}	$\tilde{\sigma}_{\text{NLO}}$
Background	463.3 pb	473.9 pb	679.9 pb	685.0 pb
Interference	-3.00 pb	-1.64 pb	-4.25 pb	-2.30 pb
Signal	2.20 pb	1.15 pb	3.95 pb	1.98 pb

Table 1: Fixed order computed cross sections for background, interference and signal computed in this framework σ , compared to the cross sections $\tilde{\sigma}$ [1].

By rescaling the effective field operator coefficients with a complex factor $(a + bi)$, not only the relative phase gets shifted but also the absolute value of the coefficients change. In this case, pure signal cross sections at LO and NLO vary by a factor of 2. As the coefficient C_{AG} enters the calculation with its square amplitude, the absolute value of the factor $(a + bi)$ seems to be too high by a factor of $\sqrt{2}$.

If the argument of the complex factor perfectly described the absorptive part of the top loop, the values for the interference should only vary by this factor of $\sqrt{2}$. As the difference is clearly higher, neither absolute value nor argument of the default phase is describing this benchmark in an accurate way.

In order to obtain accurate NLO improved results, one would have to calculate the phase factor as described in Section 3.2 and perform an event-by-event Born-reweighting [5].

5 Conclusion

In the interest of studying next-to-leading corrections to the signal and interference line-shapes of heavy scalar resonance top pair production, an effective field theory approach has been tested. An automated computational environment has been set up to generate and simulate events using MADGRAPH5_AMC@NLO and the UFO model A $\overline{\text{H}}\text{ttbar}$.

The setup was used to generate pseudoscalar resonances decaying to top quark pairs at LO and NLO to study the influence of signal and interference on the lineshape shown. At both orders of perturbation, the characteristic peak-dip structure of the interference lineshape could be reproduced.

The computed values for the cross sections of both signal and interference differ from comparable results shown by *Franzosi et al.* [1]. This might most likely be caused by using the default phase given by the UFO model leading to behaviour of the top loop different from the exact calculation. Depending on the masses, widths and couplings of the interacting particles and the total center-of-mass energy, the top-loop absorptive contribution in the ggH -vertex changes and the phase needs to be adapted accordingly.

In future event generation it should be considered to concentrate on the phase calculation required by the EFT approach. Determining the right phase factor and doing an event-by-event Born-reweighting is essential for making precise and accurate predictions.

6 Acknowledgements

I would like to give special thanks to my supervisor Alexander Grohsjean for supporting me throughout the summer student program, for introducing me to the world of particle physics and for all the interesting discussions we had concerning the project.

Thanks also to the "Lupe" group, Ceren Güzelgün, Lorenzo de Cilladi, Marco Costa and Meadhbh Murphy for the encouraging words when things were not quite working out and the valuable feedback when rehearsing for the presentation.

References

- [1] D. Franzosi, E. Vryonidou, and C. Zhang. Scalar production and decay to top quarks including interference effects at NLO in QCD in an EFT approach. [[1707.06760](#)].
- [2] **ATLAS collaboration**. Observation of a New Particle in the Search for the Standard Model Higgs Boson with the ATLAS Detector at the LHC. [[1207.7214](#)].
- [3] **CMS collaboration**. Observation of a new boson at a mass of 125 GeV with the CMS experiment at the LHC. [[1207.7235](#)].
- [4] G. Branco, P. Ferreira, L. Lavoura, M. Rebelo, M. Sher, and J. Silva. Theory and phenomenology of the two-Higgs-doublet models. [[1106.0034](#)].
- [5] O. Mattelaer. On the maximal use of Monte Carlo samples: re-weighting events at NLO accuracy. [[1607.00763](#)].
- [6] J. Alwall, R. Frederix, S. Frixione, V. Hirschi, F. Maltoni, O. Mattelaer, H. S. Shao, T. Stelzer, P. Torrielli, and M. Zaro. The automated computation of tree-level and next-to-leading order differential cross sections, and their matching to parton shower simulations. [[1405.0301](#)].
- [7] P. de Aquino, W. Link, F. Maltoni, O. Mattelaer, and T. Stelzer. ALOHA: Automatic Libraries Of Helicity Amplitudes for Feynman diagram computations. [[1108.2041](#)].
- [8] J. Alwall, C. Duhr, B. Fuks, O. Mattelaer, D. Öztürk, and C.-H. Shen. Computing decay rates for new physics theories with FEYNRULES and MadGraph5_aMC@NLO. [[1402.1178](#)].
- [9] P. Artoisenet, R. Frederix, O. Mattelaer, and R. Rietkerk. Automatic spin-entangled decays of heavy resonances in Monte Carlo simulations. [[1212.3460](#)].
- [10] A. Djouadi, J. Ellis, and J. Quevillon. Interference Effects in the Decays of Spin-Zero Resonances into $\gamma\gamma$ and $t\bar{t}$. [[1605.00542](#)].
- [11] R. D. Ball, V. Bertone, S. Carrazza, C. S. Deans, L. Del Debbio, S. Forte, A. Guffanti, N. P. Hartland, J. I. Latorre, J. Rojo, and M. Ubiali. Parton distributions for the LHC Run II. [[1410.8849](#)].
- [12] A. Denner and S. Dittmaier. The complex-mass scheme for perturbative calculations with unstable particles. [[0605312](#)].
- [13] A. Buckley, J. Butterworth, D. Grellscheid, H. Hoeth, L. Lonnblad, J. Monk, H. Schulz, and F. Siegert. Rivet user manual. [[1003.0694](#)].